2,2'-Bipyridine Complexes.   I.   Polarized Crystal Spectra of Tris(2,2'-bipyridine)copper(II), -nickel(II), -cobalt(II), -iron(II), and -ruthenium(II)[1a]

BY R. A. PALMER[1b] AND T. S. PIPER[1c]

Received August 26, 1965

The electronic spectra of the 2,2'-bipyridine (bipy) complexes of the type $M(bipy)_3{}^{2+}$ are reported for the transition metal ions Cu(II), Ni(II), Co(II), Fe(II), and Ru(II).   Polarized optical spectra of single crystals were obtained using the hexagonal crystal $M(bipy)_3Br_2 \cdot 6H_2O$ and the monoclinic crystal $M(bipy)_3SO_4 \cdot 7H_2O$.   Both pure crystals and those diluted with Zn(II) were used.   For the nickel and cobalt complexes Dq was found to be 1280 and 1270 cm^{-1}, respectively, while B was found to be 710 and 790 cm^{-1}.   Trigonal splitting in these ions is apparently quite low judging from the small differences in band maxima in parallel and perpendicular components. $Cu(bipy)_3{}^{2+}$ gives rise to a band ν_1 at 6400 cm^{-1} allowed in the perpendicular polarization ($\perp C_3$) and a second band ν_2 at 14,400 cm^{-1} allowed in both polarizations ($\perp, \parallel C_3$).   Constancy of the spectra in solutions and various crystals indicates that the complex is probably trigonal in all environments and that the strong Jahn–Teller forces are overcome by the rigidity of the ligand.   The polarization data indicate that the assignments are $^2E \rightarrow {}^2A_2$ for ν_1 and $^2E \rightarrow {}^2E$ for ν_2 and further that Dq is about 1170 cm^{-1} while K is -2600 cm^{-1}, an extraordinarily large value.   Although these assignments are based on trigonal symmetry, the hypothesis of an octahedral field with a strong tetragonal component cannot be completely ruled out and obtains some support from electron spin resonance data.   In the case of $Fe(bipy)_3{}^{2+}$, a careful search was made for the d–d spectrum.   Except for a shoulder at 11,500 cm^{-1} ($^1A_1 \rightarrow {}^3T_1$?), it was concluded that the d–d spectrum is obscured by the intense charge-transfer spectrum.   The data are consistent with a substantial increase in Dq upon spin pairing.   The most likely value in the spin-paired complex appears to be between 1650 and 1900 cm^{-1}.

Introduction

Single crystal techniques for the study of the absorption spectra of transition metal ions in trigonal ligand fields have been applied to the trisoxalates,[2] the trisacetylacetonates,[3] the trisethylenediamines,[4,5] and the trismalonates.[6]

In order to broaden and extend these investigations and to test the applicability of the ideas developed therein we began a series of studies of the tris(2,2'-bipyridine) (bipy) chelates of divalent and trivalent transition metal ions.   In this paper we report our spectral results for the divalent ions $Cu(bipy)_3{}^{2+}$, $Ni(bipy)_3{}^{2+}$, $Co(bipy)_3{}^{2+}$, $Fe(bipy)_3{}^{2+}$, and $Ru(bipy)_3{}^{2+}$. We hope in subsequent papers to report our work on the circular dichroism, electron spin resonance, and molecular orbital theory of these compounds.

The chemistry of these compounds and of other complexes of 2,2'-bipyridine and of related ligands containing the methine group has been thoroughly reviewed by Brandt, Dwyer, and Gyarfas.[7]   In addition to the intrinsic appeal of these diimine complexes, their connection with biological systems as enzyme inhibitors and models for such species as the metalloporphins has stimulated their extensive investiga-

tion by a variety of techniques.   We shall limit ourselves here to a brief review of the references most pertinent to the tris(2,2'-bipyridine) complexes and the interpretation of their electronic spectra.

The X-ray crystal structure of free 2,2'-bipyridine has been determined[8,9] and its configuration in solution deduced[10,11] from dipole moment and ultraviolet spectral data.   Crystallographic investigations of bipyridine complexes include the classic morphological work of Jaeger and van Dijk[12] as well as more recent X-ray reports on $Ni(bipy)_3SO_4 \cdot 7H_2O$,[13] $[Cu(bipy)_2]I$,[14] $Cu(bipy)_3Cl_2 \cdot 7H_2O$,[15] and the zerovalent complexes $M(bipy)_3$ of titanium, vanadium, and chromium.[16]   The magnetic moments of the trisbipyridine complexes of iron(II) and ruthenium(II) indicate spin pairing and $^1A_1$ ground states, whereas the nickel(II) and cobalt(II) complexes are spin-free.[17]   The copper(II) complex is magnetically normal.[18]   Thermodynamic properties of the first transition row divalent complexes have been thoroughly investigated by several authors.[19–22]   The infrared spectra of these compounds

(1) (a) Abstracted in part from the Ph.D. thesis of R. A. Palmer, University of Illinois, 1965.   Presented in part at the 149th National Meeting of the American Chemical Society at Detroit, Mich., April 1965.   (b) Kemisk Laboratorium IV, H. C. Ørsted Institute, Universitetsparken 5, Copenhagen, Denmark;   after July 1, 1966, Chemistry Department, Duke University, Durham, N. C. 27706.   (c) Deceased, Aug 11, 1965.   This paper was completed for submission just prior to Professor Piper's untimely death.

(2) T. S. Piper and R. L. Carlin, *J. Chem. Phys.*, **35**, 1809 (1961).

(3) T. S. Piper and R. L. Carlin, *Inorg. Chem.*, **2**, 260 (1963).

(4) A. G. Karipides, Ph.D. Thesis, University of Illinois, 1964.

(5) A. G. Karipides and T. S. Piper, *J. Chem. Phys.*, **40**, 674 (1964).

(6) W. E. Hatfield, *Inorg. Chem.*, **3**, 605 (1964).

(7) W. W. Brandt, F. P. Dwyer, and E. C. Gyarfas, *Chem. Rev.*, **54**, 959 (1954).

(8) F. Bertinotti, A. M. Liquori, and R. Pirisi, *Gazz. Chim. Ital.*, **86**, 893 (1956).

(9) L. L. Merritt and E. D. Schroeder, *Acta Cryst.*, **9**, 801 (1956).

(10) C. W. N. Cumper, R. A. F. Ginman, and A. I. Vogel, *J. Chem. Soc.*, 1188 (1962).

(11) K. Nakamoto, *J. Phys. Chem.*, **64**, 1420 (1960).

(12) F. M. Jaeger and J. A. van Dijk, *Z. Anorg. Allgem. Chem.*, **227**, 273 (1936).

(13) G. Jacobs and F. Speeke, *Acta Cryst.*, **8**, 67 (1954).

(14) G. A. Barclay, B. F. Hoskins, and C. H. L. Kennard, *J. Chem. Soc.*, 5691 (1963).

(15) D. E. C. Corbridge, Ph.D. Thesis, University of Leeds, 1951.

(16) G. Albrecht, *Z. Chem.*, **3**, 182 (1963).

(17) F. M. Burstall and R. S. Nyholm, *J. Chem. Soc.*, 3570 (1952).

(18) B. N. Figgis and C. M. Harris, *ibid.*, 855 (1959).

(19) S. Cabani, G. Moretti, and E. Scoroco, *ibid.*, 88 (1962).

(20) S. Cabani and M. Landucci, *ibid.*, 278 (1962).

(21) G. Atkinson and J. E. Bauman, Jr., *Inorg. Chem.*, **1**, 900 (1962).

(22) G. Anderegg, *Helv. Chim. Acta*, **46**, 2397, 2813 (1963).

have been reported also.[23,24] Inskeep[24] points out that splittings in the spectrum of $Cu(bipy)_3(NO_3)_2$ in the 625–660 cm^{-1} region not observed for the other first row metal ion analogs give some evidence of Jahn–Teller distortion, but in the case of the complex of the more rigid 1,10-phenanthroline there is no indication of such splitting. Ultraviolet spectra[25–27] of the 1,10-phenanthroline and 2,2'-bipyridine complexes have established beyond reasonable doubt that the intense bands above 30,000 cm^{-1} represent the slightly shifted levels of the free ligands. The circular dichroism of the iron and nickel chelates is consistent with this assignment.[28,29]

The visible and near-infrared spectra of the 1,10-phenanthroline and 2,2'-bipyridine chelates in solution have been reviewed by Kiss and Császár[30] though little detail is given by these authors. The nickel and copper complex solution spectra have been discussed in some detail by Jørgensen.[31] The intense visible spectrum of $Fe(bipy)_3^{2+}$ and related compounds has been the subject of extensive research and discussion.[32–37] The work of Busch and Bailar[33] and of Krumholtz[34] indicates that the essential chromophore is
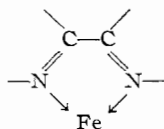
The absorption has been assigned to Laporte-allowed transitions in which the electron is excited from orbitals primarily localized on the metal to orbitals primarily localized on the ligands and π antibonding ($t_2 \rightarrow \pi^*$).[32] The similarity of the $Ru(bipy)_3^{2+}$ spectrum to that of the iron complex both in solution[38] and in crystals[39] strongly suggests a similar absorption mechanism in this complex. The ligand field spectrum of the iron complex has been assigned by König and Schläfer[40] but no analogous assignments have been made for $Ru(bipy)_3^{2+}$.

Theoretical calculations of the electronic properties of the trisbipyridine complexes include reverse crystal-field calculation of the effects of the metal ions on the ligand transitions in the ultraviolet,[26] crystal-field calculation of the d-orbital energy levels of the $Fe(bipy)_3^{2+}$ complex,[40,41] and LCAO–MO calculations of magnetic and chemical bonding properties.[42]

Experimental Section

Source and Purification of Reagents.—Commercial 2,2'-bipyridine (Columbia Organic Chemical Co., Inc.) was recrystallized once from *n*-hexane and air dried. All other chemicals were standard reagent grade. However, special precautions were taken to eliminate all traces of iron contamination in the nonferrous salts because of the enormous intensity of the visible charge-transfer bands in $Fe(bipy)_3^{2+}$. The procedure involved extracting the aqueous solutions of the simple sulfates and bromides (after addition of a few milliliters of H_2O_2) with acetylacetone in chloroform. The extraction was repeated until no trace of yellow ferric acetylacetonate appeared in the organic layer. The ruthenium trichloride used was similarly treated to remove iron contamination. The copper solutions were acidified to pH 2 to minimize the formation of $Cu(acac)_2$ and the extraction repeated about ten times. The hydrated sulfates were crystallized from water–ethanol, and the anhydrous bromides were recovered by vacuum desiccation. To be sure that all water used was also completely iron-free, a small quantity of bipyridine was added to a large container of deionized water. Just prior to use water was drawn from this container through a column of Dowex-50 cation-exchange resin, any persistent iron being retained on the column as $Fe(bipy)_3^{2+}$.

Preparation of Complexes.—The complexes whose spectra are described here were all prepared by standard methods[12] with one exception. $Ru(bipy)_3^{2+}$ was prepared by a procedure suggested by Burstall[43] but disparaged by him as giving low yield. Bipyridine (20.0 g, 25% excess) and $RuCl_3 \cdot 3H_2O$ (7.0 g) were heated under reflux for 72 hr in 95% ethanol. At the end of this time the dark orange-red solution was filtered, evaporated to a small volume, and extracted with benzene. $Ru(bipy)_3^{2+}$ was then precipitated as the iodide from the diluted aqueous solution by addition of excess KI. Contrary to the previously mentioned report[43] we obtained greater than 95% yield based on $RuCl_3 \cdot 3H_2O$. This high yield and the simplicity of the procedure make this a superior preparation of $Ru(bipy)_3^{2+}$ compared to others in the literature.[43–45]

Solutions of $Co(bipy)_3SO_4$ were prepared in a completely air-free, sealed cell. The three reactants, water, bipyridine, and $CoSO_4 \cdot 6H_2O$, were maintained in separate compartments during the deaerating and pumping down operations and mixed only after the cell and side compartments were completely sealed.

Growth of Single Crystals.—All crystals were grown from aqueous solution. Except for that of $Fe(bipy)_3^{2+}$, the sulfate crystals, $M(bipy)_3SO_4 \cdot 7H_2O$, may be grown easily either by slow evaporation or by seeding and cooling. Single crystals of the iron salt could not be grown (as previously reported[12]). Single crystals of the analogous bromides (M = Zn, Cu, Ni, Co, Fe, and Ru) were grown successfully only by slow evaporation; seeding was invariably unsuccessful.

In order to preclude oxidation, crystals containing cobalt(II) were grown under an inert atmosphere. The dilute cobalt crystals were grown in a vacuum desiccator. The crystallizing solutions were prepared by mixing solutions of the $Zn(bipy)_3^{2+}$ and of Co^{2+} salts both previously boiled and cooled under CO_2. The crystals of the pure cobalt complex salts were grown in a completely deaerated and sealed vessel.

Orientation of Crystals.—The sulfate crystals were oriented

(23) A. A. Schilt and R. C. Taylor, *J. Inorg. Nucl. Chem.*, **9**, 211 (1959).

(24) R. G. Inskeep, *ibid.*, **24**, 763 (1962).

(25) K. Yamasaki, H. Yokoi, and K. Sone, *J. Chem. Soc. Japan, Pure Chem. Sect.*, **69**, 137 (1948).

(26) H. L. Schläfer, *Z. Physik. Chem.* (Franfurt), **8**, 373 (1956).

(27) K. Sone, P. Krumholtz, and H. Stammreich, *J. Am. Chem. Soc.*, **77**, 777 (1955).

(28) J. Hidaka and B. E. Douglas, *Inorg. Chem.*, **3**, 1180 (1964).

(29) A. J. McCaffery, S. F. Mason, and B. J. Norman, *Proc. Chem. Soc.*, 259 (1964).

(30) Á. Kiss and J. Császár, *Acta Chim. Acad. Scient. Hung.*, **38**, 405, 421 (1963).

(31) C. K. Jørgensen, *Acta Chem. Scand.*, **9**, 1362 (1955).

(32) C. K. Jørgensen, *ibid.*, **11**, 166 (1957).

(33) D. H. Busch and J. C. Bailar, Jr., *J. Am. Chem. Soc.*, **78**, 1137 (1956).

(34) P. Krumholtz, *ibid.*, **75**, 2163 (1953); *Inorg. Chem.*, **4**, 612 (1965).

(35) K. Sone, *Bull. Chem. Soc. Japan*, **25**, 1 (1952).

(36) B. R. James, M. Parris, and R. J. P. Williams, *J. Chem. Soc.*, 4630 (1961).

(37) M. A. Robinson, J. D. Curry, and D. H. Busch, *Inorg. Chem.*, **2**, 1178 (1963).

(38) W. W. Brandt and G. F. Smith, *Anal. Chem.*, **21**, 1313 (1949). The many other earlier papers of G. F. Smith on the analytical aspects of the α-diimine chelates may be found listed in ref 7.

(39) This work.

(40) E. König and H. L. Schläfer, *Z. Physik. Chem.* (Frankfurt), **34**, 355 (1962).

(41) K. Madeja and E. König, *J. Inorg. Nucl. Chem.*, **25**, 377 (1963).

(42) G. Weber, *Z. Physik. Chem.* (Leipzig), **218**, 204, 217 (1962); G. Albrecht, *Z. Chem.*, **3**, 32 (1963).

(43) F. H. Burstall, *J. Chem. Soc.*, 173 (1936).

(44) F. P. Dwyer, *J. Proc. Roy. Soc. N. S. Wales*, **83**, 134 (1949).

(45) F. P. Dwyer, J. E. Humpholetz, and R. S. Nyholm, *ibid.*, **80**, 212 (1946).

Table I
Analytical Data and Molarities of Crystals

Crystal	% C Calcd	% C Found	% N Calcd	% N Found	% H Calcd	% H Found	Density, g/ml	Concn, M
$Cu(bipy)_3Br_2 \cdot 6H_2O$	45.04	45.10	10.51	10.81	4.54	4.38	1.48	1.87
$Ni(bipy)_3Br_2 \cdot 6H_2O$	45.31	45.34	10.57	10.94	4.56	4.37	1.51	1.91
$Co(bipy)_3Br_2 \cdot 6H_2O$	45.30	45.84	10.57	10.54	4.56	4.41		
$Fe(bipy)_3Br_2 \cdot 6H_2O$	45.48	44.42	10.61	10.58	4.58	4.27	1.59	2.02
$Ru(bipy)_3Br_2 \cdot 6H_2O$	43.02	43.97	10.03	10.76	4.33	4.24		

in the spectrophotometer so that the beam was either perpendicular to the {001} plane[13] (axial spectrum, unpolarized), or parallel to this plane (orthoaxial spectrum, polarized, σ or π). The bromide crystals were oriented in the same manner with respect to the {001} plane. The crystals were mounted either on thin quartz plates or over appropriate sized holes in copper plates and masked to prevent light peaks with opaque tape or Apiezon Q putty. The alignment of the crystals was verified with the aid of a polarizing microscope using extinction directions, interference figures, and (in the sulfate crystals) observation of the incipient cleavage cracking. The mounting plates were then attached to a simple room-temperature holder or placed in the dewar flask and the crystals positioned at the focus of the Cary sample beam.

Instrumentation.—All spectra were measured with a Cary Model 14-RI recording spectrophotometer using the visible and IR-1 modes. Removal of IR-1 detector heat shield permitted use of this mode of operation to the lower limit of the monochromator. No significant stray light error was observed as a result of this modification. For the orthoaxial spectra the light was polarized by a calcite Rochon prism placed in the entrance window of the sample compartment. The purity of polarization was shown to be greater than 99.9%. An iris diaphragm and/or neutral density filters was used to attenuate the reference beam. For spectra at liquid nitrogen temperature a fused silica dewar flask was used. Solution spectra were determined in 1- and 5-cm cells using standard techniques.

Treatment of Spectral Data.—The spectra of Cu-, Ni-, Co-, Fe-, and $Ru(bipy)_3^{2+}$ diluted in $Zn(bipy)_3SO_4 \cdot 7H_2O$ or $Zn(bipy)_3$-$Br_2 \cdot 6H_2O$ were corrected by subtracting from each the spectrum taken under identical conditions of temperature, spectrophotometer settings, and polarizer orientation of a pure diluent crystal of approximately the same thickness ($\pm 10\%$). The axial spectra of the *pure* Cu-, Ni-, Co-, Fe-, and $Ru(bipy)_3Br_2 \cdot 6H_2O$ crystals were not corrected except in the 4000–9000 cm^{-1} region, where the vibrational overtones of a zinc crystal of the same thickness ($\pm 10\%$) were subtracted. Each spectrum was repeated at least twice and usually many times with different crystals, different dilutions, etc., and all reported peaks were carefully verified.

Absolute and relative strengths of the transitions giving rise to the spectral bands were determined in terms of integrated band-intensities, I, where

$$I = \int (\epsilon/\nu)\,d\nu$$

which for reasonably symmetric bands can be approximated

$$I \approx (1/\nu_{max}) \int \epsilon\,d\nu$$

The molar extinction coefficient, ϵ, has the usual significance, as indicated by the equation

$$a = \epsilon c l$$

where a is the absorbance, $-\log$ (fraction of light transmitted); c is the concentration in units of moles/liter of crystal or solution; and l is the path length in units of cm. Note that I is in units of extinction coefficient. The widths of absorption bands at half-height in absorbance are also given in the tables.

The areas of the spectral bands were measured with a planimeter and should be accurate (with the exception of the very weak bands) to $\pm 5\%$. The band envelopes of overlapping bands were

approximated by drawing in curves (1) so that at any value of ν the sum of the analyzed parts equaled the total absorbance, and (2) so that the bands approximated the normal symmetric shape of an isolated absorption band. In the figures, these resolved bands are always indicated by dotted lines. The thicknesses of the $M(bipy)_3Br_2 \cdot 6H_2O$ crystals were determined with a micrometer (± 0.01 mm).

Crystal intensities corrected to random orientation were calculated from the statistical approximation

$$\langle I_{cryst}\rangle = \frac{2}{3}I_\perp + \frac{1}{3}I_\parallel$$

The perpendicular intensities were obtained from the axial spectra of pure $M(bipy)_3Br_2 \cdot 6H_2O$ crystals and this value along with that of $I_\perp/I_\parallel$, from the orthoaxial spectra of the dilute sulfate crystals was used to estimate the parallel intensities.

Determination of Crystal Densities.—The densities of the $M(bipy)_3Br_2 \cdot 6H_2O$ crystals were determined by flotation in benzene–carbon tetrachloride–methyl iodide mixtures. The flotation liquid was saturated with bipyridine for the copper complex determination to minimize formation of $Cu(bipy)_2^{2+}$. Successive determinations in all cases agreed within 1%. Densities and molarities of the crystals are given in Table I.

X-Ray Crystallography.—The space group of the $Zn(bipy)_3$-$Br_2 \cdot 6H_2O$ crystal (hexagonal form) was determined using zirconium-filtered molybdenum radiation and standard precession camera techniques. Details of this work will be published elsewhere.[46]

Crystal Structure and Morphology

The crystal matrices chosen for this work were the sulfate and bromide of the zinc(II) complex and the bromides of the copper(II), nickel(II), cobalt(II), iron(II), and ruthenium(II) complexes. X-Ray powder patterns indicate that these latter bromides are isomorphous with their zinc analog. Single crystal X-ray and optical spectral data indicate that in the bromide crystals the $M(bipy)_3^{2+}$ ions are aligned with their C_3 axes parallel.

The bromides grow as pseudo-hexagonal plates with the interesting property of altering their structure to truly hexagonal after removal from solution. Crystals examined with a polarizing microscope immediately after removal from solution exhibit a characteristic biaxial interference figure with a small optic angle. If the crystal is dried of the mother liquor, then, over a period of 20 min to several hours depending on the humidity, the optic axial angle decreases and eventually the crystal becomes optically uniaxial. The change in optical character invariably proceeds from the edges to the center of the crystal plate. Accompanying the optical change is a loss of between one-half and one molecule of water per metal ion in addition to the initial surface moisture loss. The two processes may be

(46) R. A. Palmer, G. D. Stucky, and T. S. Piper, to be published.

clearly distinguished by controlling the humidity and correlating weight loss with the change in interference figure. However, early interstitial loss around the edges of the crystal plate coincident with the surface loss precludes more exact determination of the interstitial loss. These observations suggest that the process involves layers of loosely held water molecules parallel to the plate face which may be lost without destroying the singularity of the crystal. Analyses (Table I) and site symmetry requirements indicate that the hydration number of the hexagonal form is six. The hexagonal form of the crystals was used for spectral purposes, though no significant difference in the spectra of the two forms was observed.

Dilute solutions of $Ni(bipy)_3^{2+}$ in $Zn(bipy)_3Br_2 \cdot 6H_2O$ as well as pure crystals of $Ni(bipy)_3Br_2 \cdot 6H_2O$ show a strong polarization of the $^3A_2 \rightarrow {}^3T_1$ band with respect to the c axis of the crystal. The high polarization ratio, $I_\perp/I_\parallel$, strongly suggests alignment or virtual alignment of the C_3 axes of the $M(bipy)_3^{2+}$ ions parallel to the crystal c axis. (The electric dipole selection rules for D_3 symmetry, $A_2 \xrightarrow{\perp} E$ and $A_2 -|\rightarrow A_2$, would predict zero intensity parallel to the C_3 axes.) However, the weak intensity of the $^3A_2 \rightarrow {}^3T_1$ band of nickel appearing in the parallel polarization could be due to a lack of true alignment of the ions in the crystal. To assure that this was not the case, the space group of the uniaxial form of the zinc complex crystal was determined. The precession camera data indicate that the crystal is hexagonal, P622 or P6; $Z = 2$; $a = 13.54$ A, $c = 10.71$ A. With only two molecules per unit cell, alignment of the axes is assured. In fact, in P622 or P6 the M-$(bipy)_3^{2+}$ ions must occupy 2-fold positions of D_3 (32) or C3 (3) symmetry, respectively, with their C_3 axes parallel to the crystallographic c axis.

The tabular crystals of $Zn(bipy)_3SO_4 \cdot 7H_2O$ have been described morphologically by Jaeger and van Dijk[12] and the space group of the isomorphous nickel compound determined by Jacobs and Speeke.[13] The crystal is monoclinic C2/c; $Z = 8$; $a = 22.90$ A, $b = 14.19$ A, $c = 24.80$ A, $\beta = 117° 3'$.

Crystal spectra were taken with light transmitted parallel to the {001} plane and polarized with respect to the plane normal. This plane is easily recognized by the slight cracking which develops parallel to it after the crystal is removed from solution and which leads eventually to cleavage if the crystal is not coated with lacquer or rubber cement. Polarization data indicate that the $M(bipy)_3^{2+}$ ions are aligned with their C_3 axes perpendicular to this {001} plane. For example, the polarization ratio of the $^3A_2 \rightarrow {}^3T_1$ band of Ni-$(bipy)_3^{2+}$ in the bromide crystal with the polarizations referred to the hexagonal axis ($I_\perp/I_\parallel$ of 6.6) is exactly the same as in the sulfate crystal with the polarization referred to the normal to the {001} plane. The requirements of the space group suggest that the $M(bipy)_3^{2+}$ ions occupy the 8-fold general positions of site symmetry C_2. This is consistent with the spectral data if the C_3 axes lie perpendicular to the ab plane since their alignment will be preserved by the space group
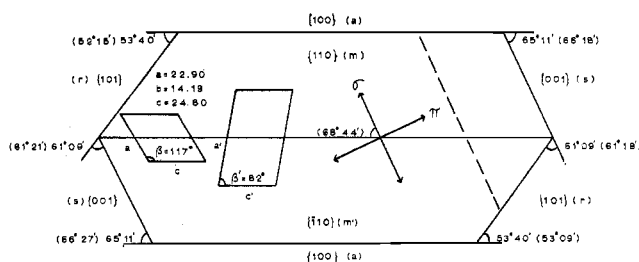

Figure 1.—Crystal morphology of $Zn(Fe,Ni,Cu)(bipy)_3 \cdot SO_4 \cdot 7H_2O$. Face indices and unprimed unit cell dimensions are those of Jacobs and Speeke[13] for the pure nickel crystal. Interfacial angles, face designations (a), (m), (r), and (s), and primed unit cell dimensions are those of Jaeger and van Dijk[12] for the zinc crystal. Angles in parentheses were experimentally determined from a dilute solid solution of copper in the zinc crystal. The dashed line indicates the cleavage plane. Colors observed with the electric vector in the π and σ directions are, respectively: light green and blue for copper, cream and red for nickel, light yellow and golden for cobalt, colorless to yellow-orange for ruthenium, and colorless and crimson for iron. π and σ are parallel and perpendicular to the normal to the cleavage plane, respectively.

operations which relate the 8-fold sites. These data and conclusions are illustrated in Figure 1.

Results

Axial Spectra.—The axial spectra of each of the $M(bipy)_3^{2+}$ ions (M = Cu, Ni, Co, Fe, and Ru) were indentical in both the pure $M(bipy)_3Br_2 \cdot 6H_2O$ crystals and in dilute solid solutions in the corresponding zinc crystal. Those data reported are for the pure crystals except for the charge-transfer peaks of $Fe(bipy)_3^{2+}$ and $Ru(bipy)_3^{2+}$. These crystal plates were generally 0.2 to 0.5 mm thick, the incident face being 2–3 mm on each edge.

It should be noted that the use of the thin plates of the bromide crystals enabled the spectra of these ions to be determined to the lower limit of the Cary 14-RI range (3333 cm^{-1}, 30,000 A). The region below 7400 cm^{-1} is not accessible in aqueous solutions owing to the absorption of the solvent. The method of obtaining the net absorption of the metal chromophore in the region between 8000 and 3333 cm^{-1} was to subtract from the absorption of the pure or dilute crystal the absorption of a $Zn(bipy)_3Br_2 \cdot 6H_2O$ crystal of the same thickness ($\pm 10\%$) taking data only in the relatively flat regions between the water and organic overtone bands. Although these bands are not appreciably altered as a function of the metal ion, their sharpness presents a practical problem of getting accurate subtraction at the peaks themselves. Taking data between the peaks avoids the scatter resulting from attempts at rigorous subtraction. Only $Cu(bipy)_3^{2+}$ of the ions investigated shows a net absorption in the region below 8000 cm^{-1}.

Orthoaxial Spectra.—The orthoaxial spectra of dilute solid solutions of the $M(bipy)_3^{2+}$ ions in single crystals of $Zn(bipy)_3SO_4 \cdot 7H_2O$ show that the σ ($\perp C_3$) and axial spectra coincide in each case. The results in the region below 8000 cm^{-1} in the sulfate spectra are not as accurate as those in the bromide crystals owing to the

overlapping of the vibrational bands. However, there is no doubt of the agreement in general features between the spectra in the two crystals.

Tris(2,2'-bipyridine)copper(II) Ion.—The axial spectrum of $Cu(bipy)_3Br_2 \cdot 6H_2O$ reveals two broad, well-resolved, comparable intense absorption bands at 14,380 and 6400 cm^{-1} (Figure 2). The orthoaxial spectrum of $Cu(bipy)_3^{2+}$ diluted in $Zn(bipy)_3SO_4 \cdot 7H_2O$ (Figures 3 and 4) is essentially the same as the axial spectrum with the electric vector of the light polarized perpendicular to the C_3 axes of the ions (σ spectrum). However, with the electric vector parallel to the C_3 axes (π spectrum), a single band is observed at 14,200 cm^{-1}. The ratio of the integrated band intensities of the perpendicular and parallel components of the higher energy band $I_\perp/I_\parallel$ is 2.72.

The effect of low temperature on the spectrum is minimal. There is a sharpening of the bands accompanied by a small increase in extinction coefficient and a slight hypsochromic shift of the higher energy band. The change in integrated band intensity of the higher energy band is small but significant (13% decrease for the $\perp$ component and a 5% increase for the $\parallel$ component). The apparent very low intensity in the lower energy region of the parallel spectrum at room temperature is reduced to zero at liquid nitrogen temperature.

The spectrum of copper(II) ion in aqueous solution saturated with bipyridine (*ca.* 6 moles of bipyridine to 1 mole of Cu^{2+}) shows the same band structure as is observed in the crystal spectrum (Figure 5). The higher energy band is shifted slightly (to 14,860 cm^{-1}) and there is some indication that the lower band is also shifted to higher energy, though the solvent absorption precludes obtaining the band maximum. With less than a 50% excess of bipyridine additional absorption in the region from 9000 to 14,000 cm^{-1} indicates the presence of other species in aqueous or alcoholic solution, notably $Cu(bipy)_2^{2+}$. Lack of appreciation of this fact probably accounts for the incorrect identification in a recent report[30] of the spectrum of primarily $Cu(bipy)_2^{2+}$ as that of $Cu(bipy)_3^{2+}$. Jørgensen[31] has given the correct aqueous solution spectrum and commented briefly on the presence and possible origin of the lower energy band, which appears not only in the tris-bipyridine complex, but in the tris(1,10-phenanthroline) complex as well.

If hydrated copper perchlorate is dissolved in nitromethane in the presence of an excess of bipyridine, the resulting spectrum is identical with that of $Cu(bipy)_3^{2+}$ in water except that the lower energy band is completely observable and the upper band is shifted to slightly lower energy (Figure 6). Dehydration of the nitromethane solution with molecular sieves until the strong combination band of H$_2$O ($\nu_1 + \nu_2$) at 5260 cm^{-1} is no longer detected has no effect on the copper spectrum. The tetraphenylborate gives the same result as does the perchlorate. The band maxima and intensities of the $Cu(bipy)_3^{2+}$ spectrum are summarized in Tables II and III.
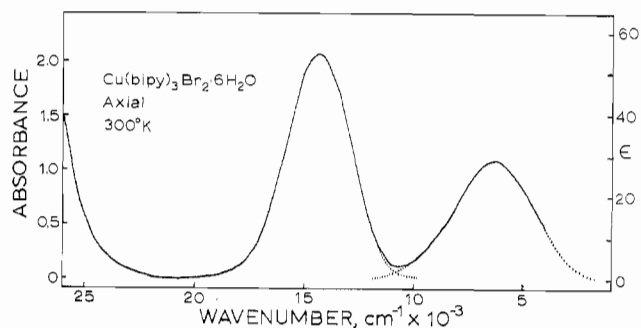

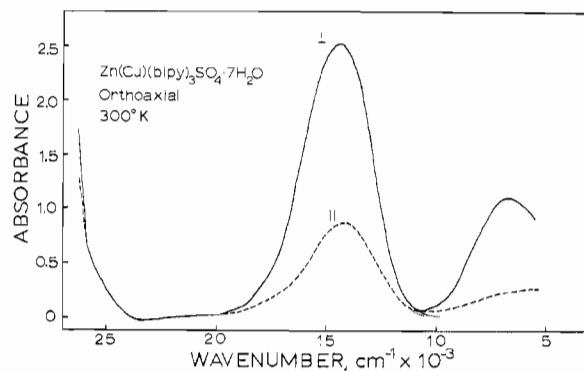Figure 2.—Crystal thickness, 0.20 mm.

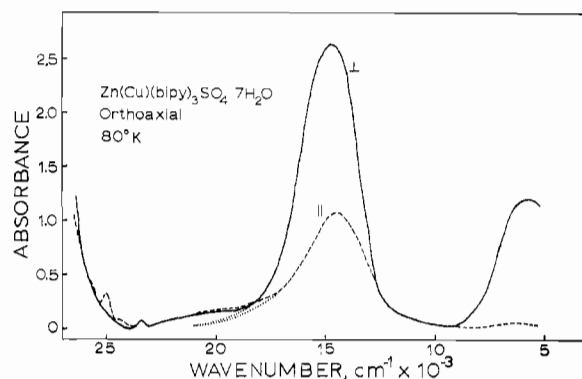Figure 3.—Crystal thickness, 2.9 mm; approximately 15 mole % copper.

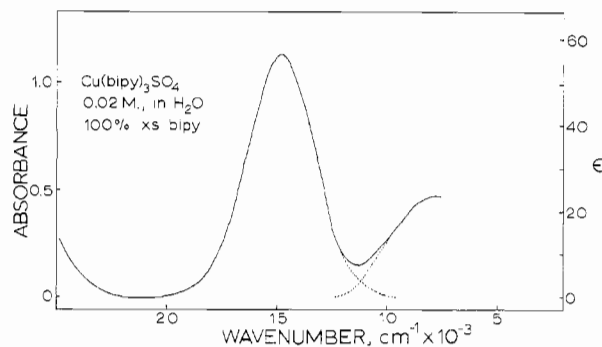Figure 4.—Crystal thickness, 2.9 mm; approximately 15 mole % copper.

Figure 5.—Path length, 1.0 cm.

Comparison of solution and average crystal intensities for the two bands (Table X) reveals slightly higher intensities in solution than in the crystal. Going from crystal to solution the higher band increases from 11.1 to 14.3 (29%) and the lower band from 12.3 to 14.4 (17%).

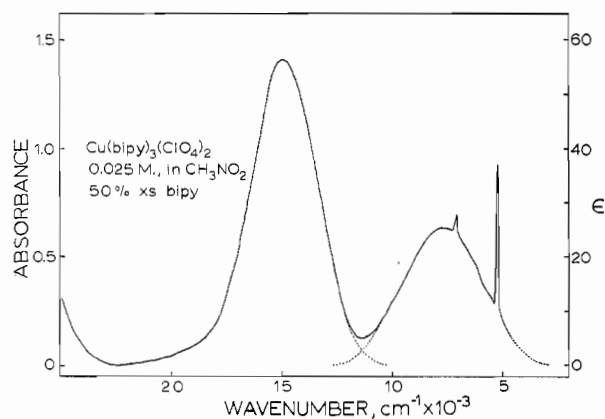**Tris(2,2'-bipyridine)nickel(II) Ion.**—The crystal

Figure 6.—Path length, 1.0 cm. Spikes of the low-energy band are water overtones appearing in the spectrum of the undried solution.

TABLE II

BAND MAXIMA OF Cu(bipy)$_3{}^{2+}$ SPECTRA

Matrix	Spectrum	Excited state	Band maxima, cm^{-1} 300°K	80°K
Cu(bipy)$_3$Br$_2$·6H$_2$O	Axial	$^2E(\perp)$	14,400	14,700
		$^2A_1$	6,400	6,400
Zn(bipy)$_3$Br$_2$·6H$_2$O	Axial	$^2E(\perp)$	14,300	14,800
		$^2A_1$	6,400	6,400
Zn(bipy)$_3$SO$_4$·7H$_2$O	σ	$^2E(\perp)$	14,400	14,800
		$^2A_1$	6,500	5,800[a]
	π	$^2E(\|\|)$	14,200	14,500
0.02 M in H$_2$O	Solution	^2E	14,860	
		$^2A_1$	7,700	
0.025 M in CH$_3$NO$_2$	Solution			
[B(C$_6$H$_5$)$_4$]$^-$		^2E	14,750	
		$^2A_1$	7,700	
ClO$_4{}^-$		^2E	14,900	
		$^2A_1$	7,700	

[a] Uncertainty of ±300 cm^1 owing to strong OH and CH overtones in the thicker crystals.

TABLE III

ABSOLUTE INTENSITIES OF Cu(bipy)$_3{}^{2+}$ SPECTRA, 300°K

Matrix, spectrum	Excited state	Width, cm^{-1}	ϵ	I
Cu(bipy)$_3$Br$_2$·6H$_2$O,	$^2E(\perp)$	3550	54.4	14.1
axial	$^2A_1$	4100	28.2	18.5
0.02 M H$_2$O, soln	^2E	3700	56.5	14.7
	$^2A_1$	4000	25	14
0.025 M CH$_2$NO$_2$, soln	^2E	3500	56.2	14.3
	$^2A_1$	4500	25.2	14.4

spectra of Ni(bipy)$_3{}^{2+}$ (Figures 7 and 8) show the same general features as does the aqueous solution spectrum.[31] There are only small differences between solution and orientation-averaged crystal intensities for both bands (Table X). The d–d transition band maxima and absolute intensities are summarized in Tables IV and V.

The temperature dependence of the intensities as shown in Figure 7 is quite low; I [$^3E(^3T_1)$] decreases 16% and I [$^3E(^3T_2)$] remains unchanged as the temperature decreases from 300 to 80°K. In addition to the polarization and temperature dependence data the low-temperature crystal spectra also reveal the presence of a weak spike at 20,960 cm^{-1} and a narrow shoulder at about 23,000 cm^{-1}, neither of which is observed in solution.
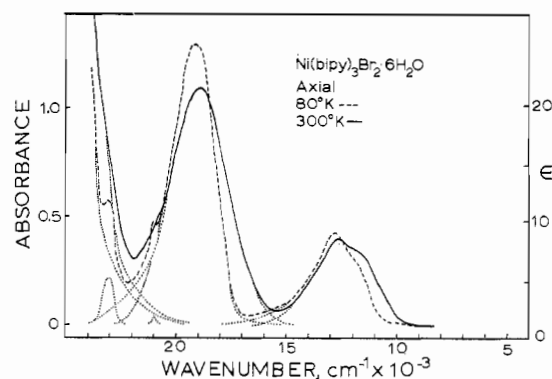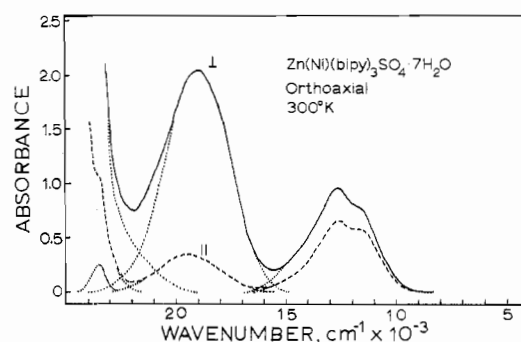

Figure 7.—Crystal thickness, 0.28 mm.

Figure 8.—Crystal thickness, 3.4 mm; approximately 25 mole % nickel.

TABLE IV

BAND MAXIMA OF Ni(bipy)$_3{}^{2+}$

Matrix	Spectrum	Excited state	Band maxima, cm^{-1} [a] 300°K	80°K
Ni(bipy)$_3$Br$_2$·6H$_2$O	Axial	$^1A_1$	(21,000)	20,960
		$^3E(^3T_1)$	18,870	19,120
		$^3E(^3T_2)$	12,740	12,820
		^1E	(11,400)	(11,700)
Zn(bipy)$_3$Br$_2$·6H$_2$O	Axial	$^1A_1$	...	20,920
		$^3E(^3T_1)$	18,870	19,100
		$^3E(^3T_2)$	12,690	12,850
		^1E	(11,690)	(11,760)
Zn(bipy)$_3$SO$_4$·7H$_2$O	σ	$^1A_1$	...	(20,800)
		$^3E(^3T_1)$	19,040	19,410
		$^3E(^3T_2)$	12,740	12,800
		^1E	(11,400)	(11,800)
	π	$^1A_1$	...	(21,000)
		$^3A_2(^3T_1)$	19,600	20,100
		$^3A_1(^3T_2)$	12,660	12,750
		^1E	(11,400)	(11,900)
0.129 M in H$_2$O	Solution	$^3T_1$	19,200	
		$^3T_2$	12,650	
		^1E	(11,900)	

[a] Bands appearing as unresolved shoulders are enclosed in parentheses.

Tris(2,2'-bipyridine)cobalt(II) Ion.—The crystal and solution spectra of Co(bipy)$_3{}^{2+}$ are illustrated in Figures 9–13, and the band maxima, extinction coefficients, and integrated band intensities are summarized in Tables VI and VII. The intensity of the band at *ca.* 11,000 cm^{-1} shows little temperature or medium dependence (Tables VII and X). However, the band maximum does exhibit considerable medium dependence and the usual hypsochromic shift at low temperature. The polarization ratio of this band $I_\perp/I_\|$ is 2.58, but

TABLE V

ABSOLUTE INTENSITIES OF Ni(bipy)$_3^{2+}$ SPECTRA

Matrix, spectrum	Excited state	Width, cm^{-1}	ϵ	I
Ni(bipy)$_3$Br$_2\cdot$6H$_2$O,	$^1A_1$	400	0.2	0.01
axial, 300°K	$^3E(^3T_1)$	3000	20.7	3.7
	$^3E(^3T_2)$	2500	6.7	1.57 } 1.8^a
	^1E	1700	2.1	0.4
80°K	$^1A_1$	100	0.8	0.01
	$^3E(^3T_1)$	2300	23.9	3.1
	$^3E(^3T_2)$	2100	7.8	1.6 } 1.8^a
	^1E	1000	1.7	0.2
0.129 M in H$_2$O, 300°K	$^3T_1$	3600	11.0	2.18
	$^3T_2 + {}^1E$	3400	7.1	2.09^a

^{a} Determined for total band using average ν_{max}.

Figure 12.—Path length, 1.0 cm.
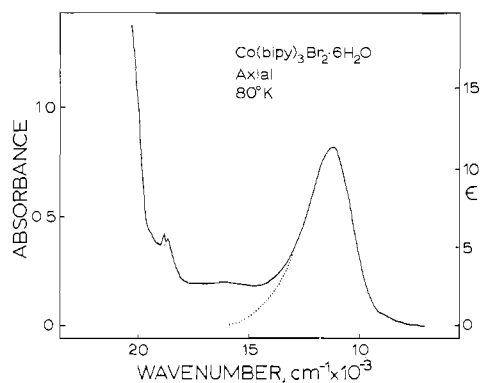

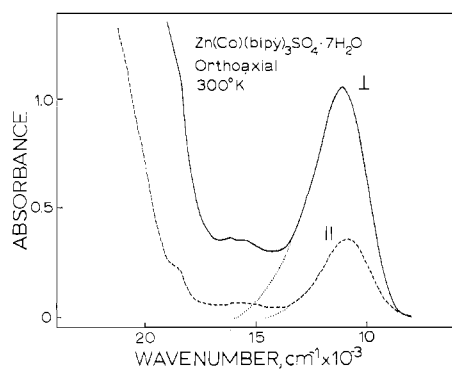Figure 9.—Crystal thickness, 0.38 mm.

Figure 13.—Detail from Figure 11.

Figure 10.—Crystal thickness, 3.8 mm; approximately 20 mole % cobalt.
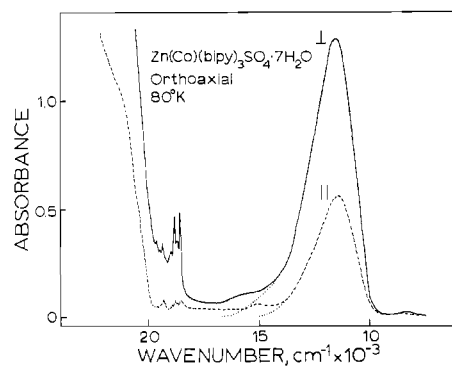
Figure 11.—Crystal thickness, 3.8 mm; approximately 20 mole % cobalt.

TABLE VI

BAND MAXIMA OF Co(bipy)$_3^{2+}$ SPECTRA

Matrix	Spectrum	Excited state	Band maxima, cm^{-1} 300°K	80°K
Co(bipy)$_3$Br$_2\cdot$6H$_2$O	Axial	$^4T_1(P)$	22,000	...
		$^2T_1(P,H)$	18,500	19,330
				19,000
				18,800
				18,600
		$^2T_1, {}^2T_2(G)$	16,000	16,000
		$^4T_2(F)$	11,000	11,350
Zn(bipy)$_3$SO$_4\cdot$7H$_2$O	σ	$^4T_1(P)$	22,000	...
		$^2T_1(P,H)$	18,700	19,750
				19,604
				19,474
				19,331
				19,220
				18,964
				18,814
				18,699
				18,554
				18,450
		$^2T_1, {}^2T_2(G)$	16,000	16,000
		$^4T_2(F)$	11,100	11,490
	π	$^4T_1(P)$	21,500	...
				19,327
		$^2T_1(P,H)$	18,700	18,939
				18,808
				18,692
				18,563
		$^2T_1, {}^2T_2(G)$	16,000	16,000
		$^4T_2(F)$	10,950	11,490
0.14 M in H$_2$O	Solution	$^4T_2(F)$	11,260	...

no evidence of trigonal splitting is observed. This is particularly evident in the 80°K spectrum.

The shoulder which is clearly evident in the crystal spectra at 22,000 cm^{-1} appears to be almost completely
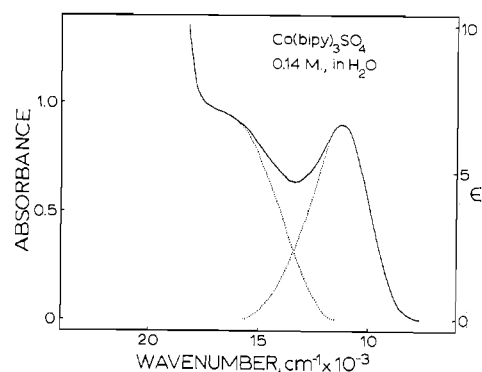
TABLE VII

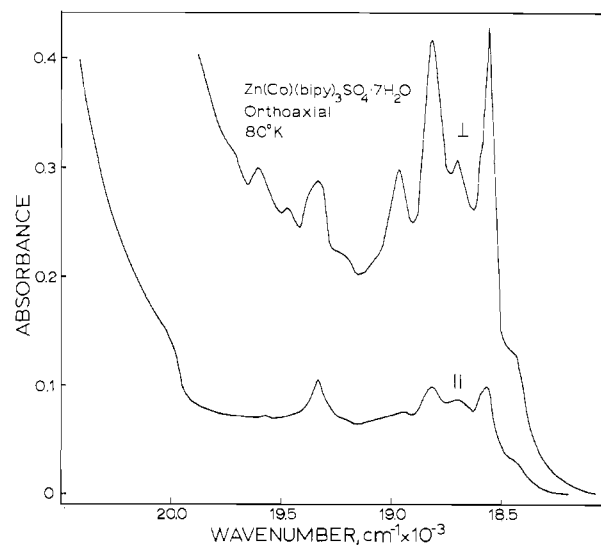ABSOLUTE INTENSITIES OF Co(bipy)$_3^{2+}$ SPECTRA

Matrix, spectrum	Excited state	Width, cm^{-1}	ϵ	I
Co(bipy)$_3$Br$_2 \cdot$6H$_2$O,				
axial, 300°K	$^4T_1(P)$	?	50	?
	$^4T_2(F)$	3200	9.20	2.88
80°K	$^2T_1(P,H)$	50–100	0.5–1.5	0.005–0.02
	$^4T_2(F)$	2500	11.36	2.79
0.14 M H$_2$O, soln	$^4T_2(F)$	3100	6.42	1.88

forbidden in the parallel polarization. However, its mergence with the charge-transfer spectrum makes assessment of its energy and intensity uncertain.

In the region between the two above bands the crystal and solution spectra are quite different. A strong broad band centered at approximately 16,000 cm^{-1} in the solution spectrum is not observed in the crystal except as it may account for some of the weak unresolved absorption between 14,000 and 18,000 cm^{-1} evident especially in the perpendicular spectrum. The appearance of this band in solution completely masks the small shoulder seen in the crystal spectrum at 18,700 cm^{-1}. At 80°K this shoulder is resolved into a number of very sharp bands with maxima between 18,450 and 19,604 cm^{-1} which are more intense in the axial spectrum (pure Co(bipy)$_3$Br$_2 \cdot$6H$_2$O) and the σ spectrum than in the π spectrum.

Tris(2,2′-bipyridine)iron(II) Ion.—The crystal spectral data for Fe(bipy)$_3^{2+}$ are summarized in Tables VIII and IX, and sample spectra are given in Figures 14–18. In Figures 17 and 18 the weak band at 8890 cm^{-1} has been retained for comparison purposes, though it is not part of the electronic spectrum (*vide infra*) and has been subtracted with the blank in all the other spectra shown. Because of the extremely high intensity of the visible absorption only the spectrum below 15,000 cm^{-1} could be measured in the pure crystal. The low-temperature spectra of the dilute crystals reveal a number of moderately intense shoulders in the visible region. These are resolved into separate components for the ⊥ spectrum in Figure 14 and for the ∥ spectrum in Figure 16.

The polarization ratio $I_\perp/I_\parallel$ of the predominant bands in the visible is 11.4 and 10.5 at 300 and 80°K, respectively. Because of the difficulty of measuring accurately the intensities of the weak parallel components, these are probably lower limits. The intensity of these bands increases by approximately 20% as the temperature decreases from 300 to 80°K.

Tris(2,2′-bipyridine)ruthenium(II) Ion.—The visible spectrum of Ru(bipy)$_3^{2+}$ (Figure 19) is very similar to that of Fe(bipy)$_3^{2+}$ in both crystal and solution. The entire spectrum is shifted about 2700 cm^{-1} to higher energy relative to that of the iron complex; other than this, the only other significant difference appears to be the absence in the ruthenium spectrum of a weak shoulder corresponding to the Fe(bipy)$_3^{2+}$ band at 11,500 cm^{-1}. (There is a shoulder at 18,000 cm^{-1}, but its extinction coefficient is much greater than that of the iron band. It seems likely that this is not a d–d

TABLE VIII

BAND MAXIMA OF Fe(bipy)$_3^{2+}$ SPECTRA

Matrix	Spectrum	Excited state[a]	Band maxima, cm^{-1} 300°K	Band maxima, cm^{-1} 80°K
Fe(bipy)$_3$Br$_2 \cdot$6H$_2$O	Axial	^3T	11,500	11,500
	σ	^3T	11,500	11,500
Zn(bipy)$_3$Br$_2 \cdot$6H$_2$O	Axial	CT-1	25,500	25,500
		CT-2	24,400	24,400
		CT-3	. . .	22,900
		CT-4	22,000	21,900
		CT-5	20,200	20,370
		CT-6	18,760	18,760
Zn(bipy)$_3$SO$_4 \cdot$7H$_2$O	σ	CT-1	. . .	25,500
		CT-2	24,500	24,200
		CT-3	. . .	. . .
		CT-4	22,000	21,600
		CT-5	20,200	20,280
		CT-6	18,870	18,690
	π	CT-7	26,300	25,500
		CT-8	23,500	23,900 / 23,260
		CT-9	. . .	22,000
		CT-10	20,410	20,200
		CT-11	18,870	18,800

[a] CT ≡ charge transfer.

TABLE IX

ABSOLUTE INTENSITIES OF Fe(bipy)$_3^{2+}$ SPECTRA, 300°K

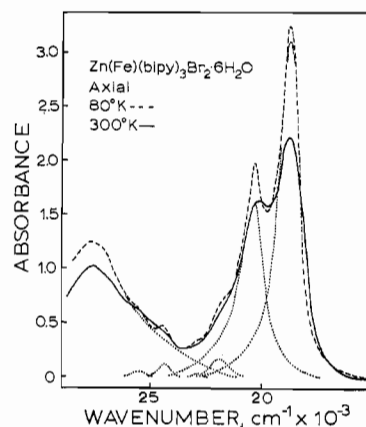| Matrix, spectrum	Excited state	Width, cm^{-1}	ϵ	I
Fe(bipy)$_3$Br$_2 \cdot$6H$_2$O,				
axial	$^3T(\perp)$	3800	3.9	1.3
σ	$^3T(\perp)$	3800	4.4	1.5
0.5 M H$_2$O soln	^3T	3800	3.6	1.1

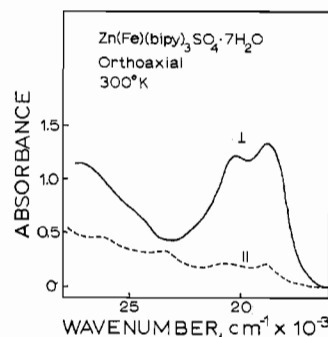Figure 14.—Crystal thickness, 0.33 mm; approximately 0.1 mole % iron.

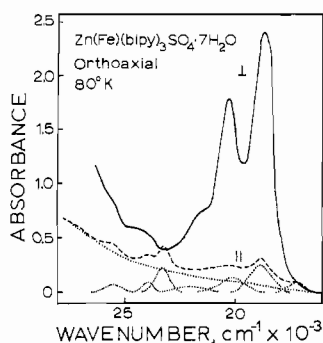Figure 15.—Crystal thickness, 1.9 mm; approximately 4 × 10^{-3} mole % iron.

Figure 16.—Crystal thickness, 1.9 mm; approximately 4 × 10^{-3} mole % iron. Dotted curves are analysis of parallel spectrum only.
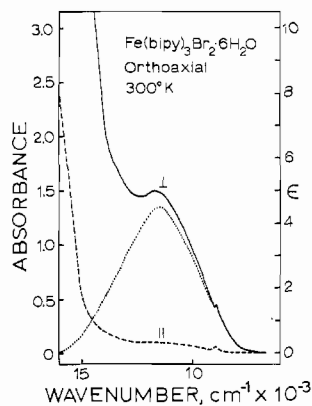

Figure 17.—Crystal thickness, 1.5 mm.
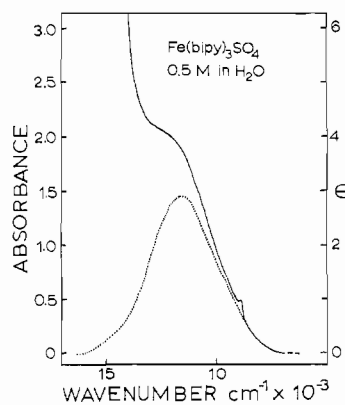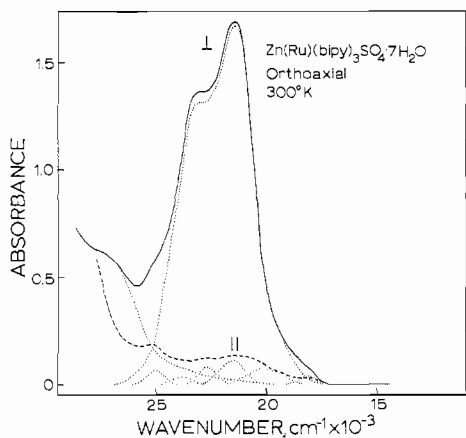

Figure 18.—Path length, 1.0 cm.

Figure 19.—Crystal thickness, 2.0 mm; approximately 2 × 10^{-4} mole % ruthenium.

TABLE X

COMPARISON OF ABSOLUTE INTENSITIES
FROM SOLUTION AND CRYSTAL SPECTRA

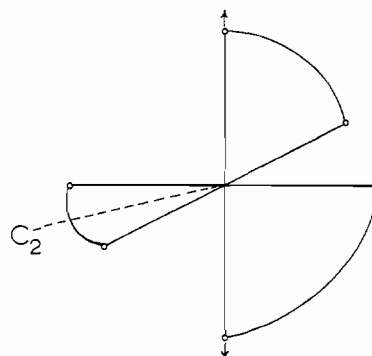| Ion	Excited state	ϵ	ϵ_{soln}	$I_\perp$	$I_\perp/I_\parallel$	$I_\parallel$	$\langle I_{cryst}\rangle$	I_{soln}
Cu(bipy)$_3{}^{2+}$	^2E	54.4	56.5	14.1	2.72	5.2	11.1	14.3
	$^2A_1$	28.2	...	18.5	→ ∞	0	12.3	14.4
Ni(bipy)$_3{}^{2+}$	$^3T_1(F)$	20.7	11.0	3.7	6.60	0.56	2.55	2.18
	$^3T_2(F)$	7.5	7.1	1.8	1.53	1.2	1.6	2.09
Co(bipy)$_3{}^{2+}$	$^4T_2(F)$	9.2	6.4	2.79	2.58	1.08	2.22	2.17
Fe(bipy)$_3{}^{2+}$	^3T	4.2	3.6	1.4	→ ∞	0	0.93	1.1

Figure 20.—A possible "tetragonal" distortion of an otherwise trigonal complex with three bidentate ligands.

band.) The polarization of the intense visible bands is almost complete with $I_\perp/I_\parallel$ being 26.5 at 300°K. The solution extinction coefficient and integrated band intensity of the intense visible doublet are 14,400 and 2430, respectively. The intensity of this doublet shows no temperature dependence between 80 and 300°.

Discussion

Tris(2,2′-bipyridine)copper(II) Ion.—Since Cu(bipy)$_3$Br$_2$·6H$_2$O is isomorphous with its zinc analog on evidence of their powder patterns, the copper ions in both of these crystals are probably at sites of either D$_3$ or C$_3$ symmetry. This is an unexpected result since the ground state of copper(II) in a trigonal field is doubly degenerate (^2E) and should be unstable according to the Jahn–Teller theorem. This orbital degeneracy is resolved in most copper compounds by a tetragonal distortion[47,48] which commonly lengthens the axial bonds by 0.2 A or more relative to the equatorial bonds and is associated with an orbital splitting of more than 10,000 cm^{-1}. It might be argued that the individual cations in Cu(bipy)$_3$Br$_2$·6H$_2$O are in fact distorted to the next lower symmetry C$_2$ and further that the distortion occurs at random along all three dihedral axes conferring upon the copper ion site a trigonal pseudo-symmetry. Note that in these chelates the commonly observed tetragonal mode involving lengthening of two Cu–N bonds *trans* to one another leaves the complex ion with that C$_2$ axis associated with the third ring in which the bond distances are unchanged; see Figure 20.

Accepting for the moment the possibility of distortion from trigonal symmetry, one would be led to predict a large distortion in solution. However, the distortion would be smaller in the pure crystal and prob-

(47) J. Bjerrum, C. J. Ballhausen, and C. K. Jørgensen, *Acta Chem. Scand.*, **8**, 1275 (1954).

(48) L. E. Orgel and J. D. Dunitz, *Nature*, **179**, 462 (1957).

ably vanishingly small in the diluent zinc crystal, because the copper ion would have to do work against the lattice forces as well as the intramolecular forces. There is considerable evidence in the case of hard crystals such as oxides that Jahn–Teller forces are ineffective against the lattice forces.[49,50] These predicted distortions should be reflected in the absorption spectra. As seen in Figures 3 and 4 and in Table II the spectrum of $Cu(bipy)_3^{2+}$ in the monoclinic sulfate crystal is essentially the same as in the pure bromide or as an impurity in the zinc bromide. The spectra in water and nitromethane show the same principal features although only the tail of the low-energy band is observable in aqueous solution owing to the light absorption of the solvent. The increase in intensity in the two bands (20–30%) going from crystal to solution (Table X) is certainly much less than would be expected for any gross structural modification. (In the case of $Cu(en)_3^{2+}$ the extinction coefficient increases by a factor of six.) The inescapable conclusion is that $Cu(bipy)_3^{2+}$ is intrinsically trigonal in both solid and solution!

An energy level diagram consistent with trigonal symmetry and the observed spectra is illustrated in Figure 21. The low temperature-dependence of the band intensities indicates that electric dipole selection rules should be effective. Since the band at 6400 cm^{-1} is strongly polarized and allowed only in perpendicular polarization we assign it to the transition $^2E \rightarrow {}^2A_1$. The band at 14,300 cm^{-1} has intensity in both polarizations consistent with our assignment to $^2E \rightarrow {}^2E$. The small splitting (200 to 300 cm^{-1}) of the perpendicular and parallel components of the ^2E band might be ascribed to a weak digonal field component, although it could also be vibronic in origin. An interpretation consistent with C_2 symmetry is also provided in the figure. The value of Dq in this interpretation of the spectrum with neglect of interaction between the two ^2E levels is 1170 cm^{-1}. This value compares quite well with that for $Ni(bipy)_3^{2+}$ (1280 cm^{-1}), but it cannot be accurate because of the large trigonal field.

There is an alternative to our energy level diagram proposed by Jørgensen,[31] who has suggested that the spectrum of $Cu(bipy)_3^{2+}$ and that of $Cu(phen)_3^{2+}$, which is identical in basic features with that of the bipyridine complex, may be interpreted in terms of a "tetragonal" distortion. In strongly tetragonal complexes such as $Cu(en)_2^{2+}$ the splitting of the octahedral ground state ^2E is so large that its upper component is found among the relatively slightly split levels of $^2T_2$ at about 14,000 cm^{-1}.[48] Jørgensen argues that the rigidity of the bipyridine and 1,10-phenanthroline ligands restricts the amount of tetragonal distortion possible in their complexes but that the splitting of ^2E should still be large enough to account for the lower
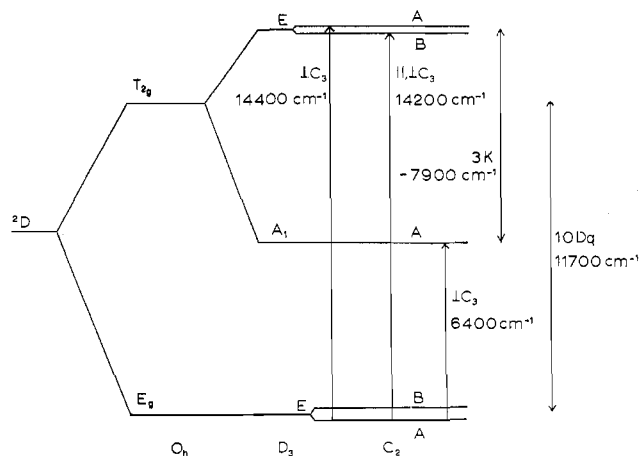

Figure 21.—Energy level diagram for $Cu(bipy)_3^{2+}$ assuming a predominantly trigonal ligand field.

energy band observed. Let us consider the polarizations predicted in this model.

Adopting the hypothesis of minimum distortion from the highest possible symmetry D_3, the Jahn–Teller instability would lead to loss of all symmetry elements except for one of the dihedral C_2 axes. An energy level diagram for this case is presented in Figure 22. Then Jørgensen's argument implies that the lower energy band at 6400 cm^{-1} would be assigned to an A $\leftrightarrow$ B transition both components of which would arise from ^2E_g (O_h). Such a transition will be allowed $\perp C_2$, *i.e.*, $\perp C_3$ *and* $\|C_3$. Since the band at 6400 cm^{-1} is allowed only in polarization $\perp C_3$, interpretation in terms of a large "tetragonal" distortion seems dubious.[51]

Returning to our energy level diagram in Figure 21, clearly its most unusual feature is the enormous trigonal splitting. K is -2600 cm^{-1}, while most known values of K lie within a few hundred wavenumbers of zero. K for $Ni(bipy)_3^{2+}$ is less than $+50$ cm^{-1}. Consistent with this large increase in trigonality is the five- to tenfold increase in intensity of $Cu(bipy)_3^{2+}$ relative to that of $Ni(bipy)_3^{2+}$.

There are three possible sources of this increased trigonality. First, the very much larger radius of copper ion relative to nickel may lead to a considerable distortion of the six nitrogens from octahedral symmetry. In molecular orbital theory the trigonality would arise in both the σ and π bonding. Second, the greater size of copper ion might allow solvation, ion pairing, and/or similar interactions to occur along the trigonal axis in both solutions and crystals. Finally, the greater electronegativity of copper ion would lead

(51) One of our experimental findings does seem to contradict the trigonal hypothesis. We have also investigated spectra of $Cu(bipy)_3^{2+}$ and $Ni(bipy)_3^{2+}$ diluted in the pseudo-hexagonal crystal $Zn(bipy)_3(IO_4)_2$. The polarization ratios for the bands in the nickel spectrum are identical with those measured for the other crystals. However, they are quite different in the case of copper. For the band with maximum at 14,400 $I_\perp/I_\|$ is 0.66 while for the band with a maximum at 6600 cm^{-1} this ratio is 0.61. The polarization ratio for the lower energy band of copper ion, which in other crystals is allowed perpendicular only, seems to support the hypothesis of pseudo-tetragonality. However, the site symmetry at the copper ion is certainly no more than C_2 and intensities can be very sensitive to small distortions. We have polarization data on $Cu(phen)_3^{2+}$ ion in crystals which are in agreement with those of $Cu(bipy)_3^{2+}$ ion in high symmetry sites. The low energy band at 6500 cm^{-1} is allowed only perpendicular while the band at 14,300 cm^{-1} is allowed in both polarizations.

(49) W. Low, *Phys. Rev.*, **109**, 256 (1958). His esr results indicate no distortions about Fe^{2+} and Co^{2+} ions in MgO.

(50) W. E. Hatfield and T. S. Piper, *Inorg. Chem.*, **3**, 1295 (1964). In this paper we estimate the Jahn–Teller forces and compare them to the force constants for distortion.
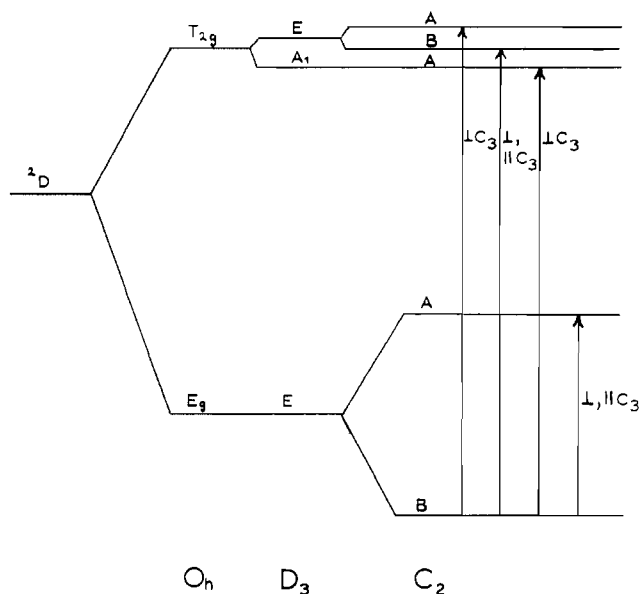
Figure 22.—Energy level diagram for $Cu(bipy)_3^{2+}$ assuming a large "tetragonal" component in the ligand field. Here the ordering of A and B components in C_2 symmetry is arbitrary.

to increased covalency in both the σ and π bonding systems.

In the ionic model, a negative value of K is associated with axial elongation (*i.e.*, contraction of the polar angle) or azimuthal contraction, the former being much more effective for small distortions. Since the angle NCuN in $[Cu(bipy)_2I]I$ is $82°$,[14] it seems that axial compression is more likely. Further, calculations with reasonable values of the radial parameters and distortional angles do not yield such a large negative K.[4] We conclude the ionic model cannot account for the trigonal splitting. Axial solvation or bonding in the crystal could account for the sign of K since the d_{z^2} orbital would be destabilized leading to a negative K. However, this idea does not seem tenable in view of the relative constancy of the band maxima in various media.

We are led then by elimination to conclude that the large trigonal splitting as well as the large band intensities must be related to a marked increase in covalency for copper as compared to the other metal ions. Whether the splitting is mainly due to π or σ covalency is not clear from these data. Indeed if there is appreciable distortion from octahedral pseudo-symmetry, there will be mixing of σ and π type states.

It is profitable here to compare the bonding tendencies of copper ion with ethylenediamine and with bipyridine. The logarithms of the stepwise formation constants are 10, 9, and -1 for ethylenediamine,[52] whereas they are 8.0, 5.6, and 3.5 for bipyridine.[22] $Cu(en)_2^{2+}$ is known to be square-coplanar, and the loss of the associated tetragonal field stabilization energy accounts for the weak bonding of the third molecule of ethylenediamine. The very different pattern of constants for bipyridine should not be taken to prove that bipyridine cannot produce strong tetragonal fields. However, solvated $Cu(bipy)_2^{2+}$ is probably *cis* octa-

hedral or trigonal bipyramidal, since *trans*-$Cu(bipy)_2$-$(H_2O)_2^{2+}$ involves considerable steric destabilization because of H–H repulsions.[53–56] These H–H repulsions are not incurred in $Cu(bipy)_3^{2+}$ whether it is trigonal or trigonal with a "tetragonal" distortion.

The stereochemistry of $Cu(en)_3^{2+}$ in aqueous solution undoubtedly involves only five nitrogens in the first coordination sphere.[52,57] However, in crystals, this ion is trigonal in the compound $Cu(en)_3SO_4$[58] and in the diluent $Zn(en)_3(NO_3)_2$.[57] Comparing this behavior of $Cu(en)_3^{2+}$ with that of $Cu(bipy)_3^{2+}$, which is probably trigonal in both solids and solution, the greater tendency of the ethylenediamine complex to distortion (and possibly solvation) is probably due to the greater flexibility of the ligand. Recalling the severe distortion of aquated copper ion, we conclude that chelation confers a considerable resistance to Jahn–Teller distortions and that chelation with a rigid ligand such as bipyridine or 1,10-phenanthroline can confer immunity to such distortions.[59]

In contrast to the consistency of the above arguments based mainly on optical spectra and crystallography, the esr data are not readily reconciled with the conclusion of essential trigonal symmetry of the $Cu(bipy)_3^{2+}$ ion. The esr spectrum of $Cu(bipy)_3(NO_3)_2$ as a crystalline powder gives a g tensor, isotropic at room temperature ($g = 2.114$) but anisotropic at $-196°$.[60] This has been interpreted[60] as indicating a sizable Jahn–Teller ("tetragonal") distortion.[61] The spectrum resembled very closely that of other tetragonal copper complexes and on this basis was analyzed in terms of a $g_\perp$ of 2.046 and a $g_\parallel$ of 2.268. Our single crystal esr data agree in general with the powder data, but show more detail and resolution. The angular dependence of the g values at $-196°$ definitely indicates the presence of a field of symmetry lower than C_3.[62] However, the X-ray and absorption spectral data indicate that such a lower symmetry field is not accompanied by appreciable nuclear displacements. If the ion were disposed to distortion of its atomic framework, certainly the spectrum would show greater energy and intensity dependence on the medium; there is little difference noted even between the solution and dilute single crystal spectra.[60] This leads us to propose that the lower symmetry field is associated with a small rhombic distortion of the electron density, imposed on the large trigonal field due to the extensive π bonding. If such be the case, the interpretation of the esr spectrum must be in terms of C_2 symmetry. It is not clear

(52) J. Bjerrum and E. J. Nielson, *Acta Chem. Scand.*, **2**, 297 (1948).

(53) F. P. Dwyer, H. A. Goodwin, and E. C. Gyarfas, *Australian J. Chem.*, **16**, 544 (1963).
(54) A. B. Ablov and D. M. Palade, *Zh. Neorgan. Khim.*, **6**, 601 (1961).
(55) E. D. MacKinzie, Ph.D. Thesis, University of New South Wales, 1962.
(56) A. M. Sargeson, private communication.
(57) T. S. Piper and A. G. Karipides, *Inorg. Chem.*, **4**, 923 (1965).
(58) M. Cola, G. Gruseppetti, and F. Mazzi, *Atti. Acad. Sci. Torino*, **96**, 38 (1962).
(59) A further example of a chelated molecule which is resistant to Jahn–Teller distortion is that of manganese acetylacetonate. See B. Morosin and J. R. Brathovde, *Acta Cryst.*, **17**, 705 (1964).
(60) H. C. Allen, G. F. Kokoszka, and R. G. Inskeep, *J. Am. Chem. Soc.*, **86**, 1023 (1964).
(61) A. D. Liehr and C. J. Ballhausen, *Ann. Phys.* (N. Y.), **3**, 304 (1958).
(62) R. A. Palmer and T. S. Piper, unpublished results.

what g values and hyperfine constants should be expected with such a field. We hope to shed further light on this question in a subsequent publication.

Tris(2,2'-bipyridine)nickel(II) Ion.—The electronic configuration of nickel(II) is d^8 and the octahedral ground state $^3A_2$.[17] The octahedral field spin-allowed d–d transitions of interest are, in order of increasing energy, $^3A_2 \rightarrow {}^3T_2(F)$, $^3T_1(F)$, and $^3T_1(P)$.[63] Transition to the $^3T_1(P)$ level, found at 29,000 cm^{-1} in Ni(en)$_3{}^{2+}$ and at 28,200 cm^{-1} in Ni(NH$_3$)$_6{}^{2+}$,[47] is apparently obscured in the Ni(bipy)$_3{}^{2+}$ spectrum by the intense broad shoulder on the ultraviolet ligand bands. The extinction coefficient of this shoulder is approximately 400 in solution.

Since the symmetry about the nickel ion is undoubtedly D$_3$, each of the triply degenerate octahedral levels will be split into an A and an E component by the trigonal field: $^3T_2 \rightarrow {}^3E + {}^3A_1$; $^3T_1 \rightarrow {}^3E + {}^3A_2$. The pertinent electric dipole selection rules in D$_3$ symmetry are then

$$A_2 \xrightarrow{\quad} A_2$$
$$A_2 \xrightarrow{\parallel} A_1$$
$$A_2 \xrightarrow{\perp} E$$
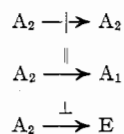
The assignment of electric dipole character to the d–d transitions made on the basis of the low temperature-dependence of the intensities is supported by the strong polarization of the $^3T_1$ band in the crystal spectra. However, the intensity in the parallel component ($^3A_2$) represents partial breakdown, presumably vibronic, of the selection rules, by which this transition should be strictly forbidden. The polarization of the $^3T_2$ band is very slight.

Energy level calculations for the d^8 configuration[63,64] indicate that two lower singlet states ($^1E(D)$ and $^1A_1(G)$) and two higher ($^1T_2(D)$ and $^1T_1(G)$) are at energies low enough to give rise to absorptions in the optical spectrum. The increased resolution in the high-energy region of the crystal spectrum at low temperatures permits the location of the $^1A_1$ level, not before observed for Ni(bipy)$_3{}^{2+}$. The small spike which appears in the axial spectrum of the pure Ni(bipy)$_3$Br$_2$·6H$_2$O crystal at 20,960 cm^{-1} ($\epsilon \approx 1.0$; $I \approx 0.01$) is assigned to this spin-forbidden transition. The peak is also observed in the perpendicular and parallel spectra but is less well resolved in the sulfate crystal due to poorer slits.

The higher energy spin-forbidden bands are not observed. The partially resolved peak which appears in the low-temperature spectra at 23,040 cm^{-1} (Figure 7) cannot be assigned to a d–d transition because of its small half-width; the spin-forbidden transition $^3A_2 \rightarrow {}^1T_1$ is a $t_2 \rightarrow e$ transition and must have a half-width of 2000–4000 cm^{-1}. The peak at 23,040 cm^{-1} may be due to a transition within the ligand, perhaps $\pi \rightarrow \pi^*$.

The assignment of the shoulder on the low-energy side of the infrared band has been the subject of some controversy. Jørgensen[31] has assigned this shoulder to the spin-forbidden transition $^3A_2 \rightarrow {}^1E$. However, Liehr and Ballhausen[64] assigned this double band to the spin–orbit components of the $^3T_2$ level. The extensive data of Busch and co-workers[37] gives considerable weight to Jørgensen's arguments in the range of higher Dq in the α-diimine chelates. In cognizance of these results we have assigned the shoulder to the ^1E transition in the crystal spectra as well.

Adopting this assignment and considering the relationship of the $^1A_1$ energy to that of the $^3T_1$ we arrive at a value of Dq/B[63] of 1.8. Using the value of Dq from the low-temperature spectrum (1279 cm^{-1}), B is 710 cm^{-1}. This represents a 31% lowering of the repulsion parameter from the free-ion value. Although this is unexpectedly low, consistency of agreement for the energies of ^1E, $^3T_2$, $^3T_1$, and $^1A_1$ with theory[63] is excellent.

Other evidence for delocalization and involvement of nonionic forces in Ni(bipy)$_3{}^{2+}$ is given by a comparison of the intensity ratios $I(^3A_1):I(^3E_a):I(^3A_2):I(^3E_b)$ with those predicted by theory. The ratios given by the ionic model are $4:1:0:2.78^4$ and for the σ-bonding molecular orbital model $4.1:1:0:1.9$,[5] whereas the values observed for Ni(bipy)$_3{}^{2+}$ are in the ratio of $0.66:1:0.31:2.06$. Since the nickel ratios are clearly in disagreement with the theoretical ratios and with those observed in the oxalates or ethylenediamines,[5] we can conclude that the intensity mechanism must be quite different and probably involves the π orbitals.

The trigonal splitting of both $^3T_2$ and $^3T_1$ is $^3/_2K$. However, owing to the apparent partial vibronic character of the bands, particularly the $^3T_2$, the small differences in band maxima shown by the parallel and perpendicular components cannot be interpreted in terms of trigonal splitting. One can only say that the trigonal splitting is probably very small.

Tris(2,2'-bipyridine)cobalt(II) Ion.—The electronic spectrum of cobalt(II) in fields of octahedral symmetry has been reported in detail both in solution and crystalline media.[49,65–71] Liehr[72] has published a complete energy level diagram for the d^7 electronic configuration in a field of octahedral symmetry including spin–orbit coupling.

Our spectra of Co(bipy)$_3{}^{2+}$ in both crystal and solution (Figures 9–12) reveal a band at 11,300 (± 300 cm^{-1} depending on medium and temperature) which we may confidently assign to the octahedral-field transition $^4T_1(F) \rightarrow {}^4T_2(F)$ consistent with other observations.[65–71] The discrepancy between this value and that of Kiss and Császár[30] is thought due to the low performance of their spectrophotometer in the 10,000 cm^{-1} region. We assign the second spin-allowed

(63) Y. Tanabe and S. Sugano, *J. Phys. Soc. Japan*, **9**, 753, 766 (1954).
(64) A. D. Liehr and C. J. Ballhausen, *Ann. Phys.* (N. Y.), **6**, 134 (1959).

(65) O. G. Holmes and D. S. McClure, *J. Chem. Phys.*, **26**, 1686 (1957).
(66) R. Pappalardo, *Phil. Mag.*, **4**, 219 (1959).
(67) G. W. Pratt, Jr., and R. Coelho, *Phys. Rev.*, **116**, 281 (1959).
(68) J. Ferguson, *J. Chem. Phys.*, **32**, 533 (1960).
(69) C. J. Ballhausen and C. K. Jørgensen, *Acta Chem. Scand.*, **9**, 397 (1955).
(70) R. Newman and R. M. Chrenko, *Phys. Rev.*, **115**, 1147 (1959).
(71) R. Pappalardo, D. L. Wood, and R. C. Linares, Jr., *J. Chem. Phys.*, **35**, 2041 (1961).
(72) A. D. Liehr, *J. Phys. Chem.*, **67**, 1314 (1963).

transition, $^4T_1(F) \rightarrow {}^4T_1(P)$, to the shoulder on the charge-transfer band at approximately 22,000 cm^{-1} in the crystal spectrum.

The assignment of the above transitions allows the calculation of the parameters Dq and B.[63] Taking 11,400 and 22,000 cm^{-1} as the respective band energies we obtain $Dq = 1267$ cm^{-1} and $B = 791$ cm^{-1}, in excellent agreement with the values (of Dq) for Ni-(bipy)$_3{}^{2+}$ (1265, solution; 1271, crystal, 300°K; 1279, crystal, 80°K) and for Cu(bipy)$_3{}^{2+}$ (1237, solution; 1170, crystal).

From the values of Dq and B the energy of the $^4T_1(F) \rightarrow {}^4A_2(F)$ transition in Co(bipy)$_3{}^{2+}$ is calculated to be 23,000 cm^{-1}. Owing to the very weak absorption[73] expected for this two-electron transition and its location between the $^4T_1(P)$ band and the onset of charge transfer, we would not expect to distinguish its effects on the spectrum.

We turn now to assignment of the weak bands in the crystal spectrum in the region between 14,000 and 20,000 cm^{-1}. The weak shoulder at 18,500 cm^{-1} is resolved at 80°K into at least eleven distinct, sharp peaks between 18,450 and 19,604 cm^{-1} (Figures 11 and 13). This coincides very closely with the energy calculated[63,72] for the $_b{}^2T_1$ level arising from the ^2P and ^2H free-ion states. Accordingly we assign these sharp bands to this transition (splittings are discussed in detail below).

The broad, low, ill-defined but unmistakable absorption in the crystal spectrum between 14,000 and 18,000 cm^{-1} is likely due to transitions to the $_a{}^2T_1(G)$ and $_a{}^2T_2(G)$[63,72] states which should also be split by the combination of spin–orbit coupling and trigonal field and may in addition be affected by vibronic interaction. However, if this assignment is correct we do not have an explanation as to why these levels do not give rise to sharp lines and progressions as does the $_b{}^2T_1$ level.

The anomalous absorption in the solution spectrum (Figure 12) centered at about 16,000 cm^{-1} cannot be explained in the context of the electronic energy levels of Co(bipy)$_3{}^{2+}$. There is no reason to suspect that any of the bands assigned above should have grossly shifted or that the $^2T_{1,2}(G)$ transitions should have increased in intensity tenfold. Further, since the solutions were saturated with bipyridine, dissociation can be discounted.[22] Considering the anaerobic conditions maintained during the preparation of the solutions and during spectral measurements, we postulate that this absorption is due to the Co(bipy)$_3{}^+$ ion, which has an intense, broad absorption band at 16,000 cm^{-1}.[74] Vlček[75] has assigned this band to a bis complex in an aqueous chloride medium. However, dissociation seems very unlikely in our solutions (*vide supra*). If the absorption at 16,000 cm^{-1} is due to Co(bipy)$_3{}^+$, the apparent extinction coefficient indicates that approximately 1% of the Co(bipy)$_3{}^{2+}$ has been reduced.

Two processes might conceivably be responsible for the presence of the univalent complex. First, reduction of Co(bipy)$_3{}^{2+}$ by bipyridine or by light, and second, disproportionation of the divalent complex to Co(bipy)$_3{}^+$ and Co(bipy)$_3{}^{3+}$ analogous to the behavior of the chromium(II)[76] and vanadium(I)[77] complexes. The polarographic half-wave potentials for the reductions of Co(bipy)$_3{}^{3+}$ to Co(bipy)$_3{}^{2+}$ and Co(bipy)$_3{}^{2+}$ to Co(bipy)$_3{}^+$ allow a rough estimate of the potential of the disproportionation reaction of -1.0 volt.[78] On this basis we may rule out disproportionation.

The close agreement of the axial and σ spectra and the small temperature dependence of the intensities gives support to an electric dipole interpretation of the spectrum. Although strong polarization effects are observed, splitting of the $^4T_2(F)$ level is not observed even at 80°K. This may be interpreted to mean that the trigonal splitting is smaller than or of the same magnitude as the spin–orbit splitting. The total first-order spin–orbit splitting of the $^4T_2$ level should be $^2/_3\zeta$ or 360 cm^{-1},[71] assuming the free-ion value of $\zeta = 540$ cm^{-1}. The trigonal field may be just large enough to completely confuse the six components predicted by the combination of spin–orbit and trigonal splitting. Spectra at 4°K should help resolve this question.

We now turn to the sharp lines in the region of 19,000 cm^{-1} (Figure 13). In an octahedral field the $_b{}^2T_1$ level ought to give rise to two levels split by the order of magnitude of ζ, the spin–orbit coupling constant.[72] In a trigonal field second-order effects will lift the degeneracy further to three Kramer's doublets. There are two lines which stand out because of their intensity; they occur at 18,554 and 18,814 cm^{-1} and are split by 260 cm^{-1}. These two lines probably arise from 0–0 transitions. It is difficult to decide whether there is another 0–0 line in this region. If there is not, the trigonal field must be quite small. In this interpretation the weak shoulder at 18,450 cm^{-1} would have to be assigned to a hot line and then each of the two strong lines would have associated with it a vibrational component at about 150 cm^{-1} above the origin. Further, the whole pattern seems to be repeated at about 780 cm^{-1} higher in energy. This is similar to that of the out-of-plane C–H deformation at 778 cm^{-1}.[79] If such a vibration were excited, serious delocalization of metal electrons onto the ligand would be implied.

If the origins are chosen on grounds other than intensity, then several different interpretations of these lines are possible. For instance, the energy of the Co–N stretch (264 cm^{-1})[24] coincides closely with several of the intervals. However, basing the assignments on coupling with this vibration leads not only to unlikely intensity relationships between components of the progressions, but to an unreasonable value of the spin–orbit coupling constant.[72]

Tris(2,2′-bipyridine)iron(II) Ion.—The assignment of the extremely intense bands in the visible spectrum of

(73) S. Koide, *Phil. Mag.*, **4**, 243 (1959).
(74) G. M. Waind and B. Martin, *J. Inorg. Nucl. Chem.*, **8**, 551 (1958).
(75) A. A. Vlček, *Z. Physik. Chem.* (Leipzig), Sonderheft, 143 (1958).

(76) F. Hein and S. Herzog, *Z. Anorg. Allgem. Chem.*, **267**, 337 (1952).
(77) S. Herzog, *Naturwissenschaften*, **43**, 35 (1956).
(78) A. A. Vlček, private communication.
(79) L. J. Bellamy, "The Infrared Spectra of Complex Molecules," John Wiley and Son, Inc., New York, N. Y., 1958.

Fe(bipy)$_3{}^{2+}$ to (t$_2$ → π*) type transitions[32] is supported by the crystal spectra. Two factors not obvious from solution spectra are significant in this regard: the narrowness of the bands and the temperature dependence of their intensities. In the low-temperature axial spectrum of the Fe(bipy)$_3{}^{2+}$ ion in the Zn(bipy)$_3$Br$_2$·6H$_2$O crystal, the half-widths of the bands are only 1100 cm^{-1} (Figure 14). At room temperature their half-widths are greater, but still less than 1500 cm^{-1}. These same band widths are also seen (Figures 14 and 16) to be characteristic of all of the less-intense bands found in the parallel and perpendicular spectra of the ion in this region. This is considerably narrower than bands of d–d transitions of the type t$_2$ → e, whose half-widths are of the order of 3000 to 4000 cm^{-1}. The increase in intensity of the bands in the visible on going to low temperatures is also atypical of crystal field bands. This increase amounts to a factor of 1.2 in the perpendicular spectrum and 1.3 in the parallel. This *is*, however, consistent with the assignment of the bands to charge transfer, since such transitions would be enhanced by the decrease in the Fe–N distance which undoubtedly occurs with decrease in temperature.

Although several bands are distinguishable in the visible spectrum (Figures 14 and 16) which might on the basis of their intensities be reasonably assigned to the d–d transitions strongly mixed with the charge–transfer bands, their half-widths are much too small (1100 to 1500 cm^{-1}). One must conclude that the crystal field spectrum of Fe(bipy)$_3{}^{2+}$ is not observed in the visible region.

The ground state of Fe(bipy)$_3{}^{2+}$ (d^6, spin-paired) is ^{1}A$_1$.[17] The d–d transitions expected in the near-infrared–visible region in order of increasing energy are:[63] ^{1}A$_{1g}$ → ^{3}T$_{1g}$, ^{3}T$_{2g}$, ^{1}T$_{1g}$, and ^{1}T$_{2g}$ in an octahedral field. The symmetry of the ion should be no lower than D$_3$ since the nondegenerate ground state does not impose any distortion requirements. The only attempt to assign d–d transitions in the Fe(bipy)$_3{}^{2+}$ spectrum has been that of König and Schläfer.[40] These authors assign one spin-allowed and both spin-forbidden transitions to extremely weak shoulders which they observe on the infrared tail of the visible charge-transfer bands in solution. (They assign another shoulder, which they observe only in Fe(phen)$_3{}^{2+}$, to the spin-allowed transition, ^{1}A$_1$ → ^{1}T$_2$.)

In the course of the work reported here on the crystal spectra of the M(bipy)$_3{}^{2+}$ ions, it early became obvious that the weak, sharp peak at 8890 cm^{-1} in the spectra of the diluent zinc crystals (Figures 15 and 16) was the same as that which König and Schläfer[40] observed at 8960 and 8980 cm^{-1} in the Fe(phen)$_3{}^{2+}$ and Fe(bipy)$_3{}^{2+}$ solution spectra, respectively. (They assign this peak to the spin-forbidden ^{1}A$_1$ → ^{3}T$_1$ transition in iron(II).) This same peak is observed in crystals and in concentrated solutions of all the trisbipyridine metal complex ions studied here and in pure crystalline bipyridine. It can be assigned with a great degree of assurance to the second overtone of the C–H stretching vibration.[80]

We were, in fact, able to verify only one electronic transition in the Fe(bipy)$_3{}^{2+}$ spectrum below 15,000 cm^{-1}. Our crystal spectra indicate that this band, which König and Schläfer[40] report at 12,100 cm^{-1}, is more properly located at 11,500 cm^{-1} (Figures 17 and 18). Its intensity shows little or no temperature dependence. It is completely polarized within experimental error, being allowed only in the perpendicular polarization.

The energy, intensity, and width of this band are compatible with its assignment to a d–d transition. Its integrated band intensity ($I = 1.4$) is somewhat less than one might expect for a spin-allowed d–d band. (The total integrated band intensities for the spin-allowed bands of Ni(bipy)$_3{}^{2+}$ are 3.0 and 4.3.) The fact that the polarization of the band follows that of the charge-transfer bands suggests the possibility of its being substantially mixed with these transitions; *e.g.*, through spin–orbit coupling. If this be the case, however, the intensity is certainly too small to be associated with a spin-allowed band. On the other hand, if there is no mixing, we must explain the polarization in terms of dielectric dipole selection rules. In D$_3$ symmetry these predict intensity in both parallel and perpendicular polarizations for ^{1}A$_1$ → ^{1}T$_1$ but only in the perpendicular for ^{1}A$_1$ → ^{1}T$_2$. Our choice then would have to be ^{1}T$_2$, since the band is completely polarized. But this would require that the ^{1}A$_1$ → ^{1}T$_1$ transition be observed at *ca.* 6000 cm^{-1}, whereas we found no comparably intense electronic transition below 11,500 cm^{-1}. Thus, based on intensity and polarization data, we conclude that this band is most likely associated with neither of the spin-allowed d–d transitions.

The intensity which might be gained by a spin-forbidden band at 11,500 cm^{-1} through coupling with the t$_2$ → π* transition at 18,800 cm^{-1} can be crudely estimated by the equation

$$I(^1A_1 \rightarrow {}^3T) \approx [I(t_2 \rightarrow \pi^*) \cdot \zeta \cdot \gamma][E(\pi^*) - E(^3T)]^{-1}$$

where ζ is the spin–orbit coupling constant and γ is the coefficient giving the amount of d-orbital character in the π* state. We estimate $I(t_2 \rightarrow \pi^*)$ to be about 900. If we assume a ζ of 100 cm^{-1} and a γ of 0.1, then the calculated intensity of the singlet–triplet transition from (A) is 1.2, which is certainly the right order of magnitude (*cf.* 1.4 experimentally observed for the perpendicular polarization).

Work on a wide variety of α-dimine complexes indicates that the mean spin pairing energy π of Fe^{2+} is 12,500 ± 800 cm^{-1}.[37] This has led to an estimate for Dq of 1330 cm^{-1} for Fe(bipy)$_3{}^{2+}$.[81] However, as Orgel[82] and later Jørgensen[83] have pointed out, the decrease in r, the metal–ligand distance, which accompanies the transfer of electron density from the e$_g$ to

(80) J. Turkevich and P. C. Stevenson, *J. Chem. Phys.*, **11**, 328 (1943), give values for the C–H stretch in pyridine of 3070 cm^{-1} in the vapor and 3077 cm^{-1} in the liquid.

(81) Madeja and König[41] arrived at a Dq value of 1311 cm^{-1} for Fe(phen)$_3{}^{2+}$ and also a value of 1190 cm^{-1} for π, although, as noted above, their band assignments are in error.

(82) L. E. Orgel, "Reports to the Tenth Solvay Council, Quelques Problèmes de Chimie Minérale," Stoops, Bruxelles, 1956, p 289.

(83) C. K. Jørgensen, "Absorption Spectra and Chemical Bonding in Complexes," Pergamon Press, Oxford, 1962, p 128.

the t_{2g} orbitals should result in a 10–20% increase in Dq per electron transferred; that is, a 10–20% increase over the value of Dq for the complex before transfer. We may take this to be the value $Dq = \pi$. It has also been observed that β should decrease with r.[84] Further, in the trisdiethyldithiocarbamates[85] β is found to go to a minimum for the cobalt(III) complex (d^6, spin-paired). In light of these observations and taking Busch's estimated limits of π,[37] we begin by assuming that Dq for Fe(bipy)$_3{}^{2+}$ is between 14,000 and 18,600 cm^{-1}; *i.e.*, 11,700 + 20% to 13,300 + 40%. As an upper limit of β we take the value found for Co(bipy)$_3{}^{2+}$, 0.75, and guess that, in fact, β for Fe(bipy)$_3{}^{2+}$ may be as low as 0.4. The free-ion value of B for Fe^{2+} is 1050 cm^{-1} and so our assumed limits for B for Fe(bipy)$_3{}^{2+}$ are 420 to 750 cm^{-1}.

The energy expressions for the d–d transitions are

$$E(^1A_1 \rightarrow {}^3T_1) = \Delta - 12B - 50B^2/\Delta - 8\alpha$$

$$E(^1A_1 \rightarrow {}^3T_2) = \Delta - 4B - 14B^2/\Delta - 8\alpha$$

$$E(^1A_1 \rightarrow {}^1T_1) = \Delta - 4B - 86B^2/\Delta - 8\alpha$$

$$E(^1A_1 \rightarrow {}^1T_2) = \Delta - 12B - 2B^2/\Delta - 8\alpha$$

where the factors kB^2/Δ include the off-diagonal elements,[86] $\pm 8\alpha$ is the appropriate Trees correction,[87] and C is assumed equal to $4B$. From these expressions we find, in support of our conclusion above, that the band at 11,500 cm^{-1} is at too low energy to be assigned to even the lower singlet–singlet transition. However, the situation as regards the singlet–triplet transitions is not resolved. For the assignment $^1A_1 \rightarrow {}^3T_1$ reasonable values of B are obtained for $16,500 < \Delta < 19,000$ cm^{-1} and for the assignment $^1A_1 \rightarrow {}^3T_2$, for $14,000 < \Delta < 14,500$ cm^{-1}. The fact that no electronic transitions were found below 11,500 cm^{-1} favors the $^3T_1$ assignment. If the other assignment were made, then the $^3T_1$ band would be expected at about 6500 cm^{-1}. Its intensity by the above crude estimate should still be 0.5, but might be much less, resulting in its going unobserved even in the pure crystals. Further work is in progress to clarify this issue.

Summary

The more important conclusions of this work are now summarized.

(1) In both crystals and solution Cu(bipy)$_3{}^{2+}$ is probably very close to trigonal symmetry despite strong Jahn–Teller forces. We postulate that rigid bidentate ligands confer considerable immunity to Jahn–Teller distortion.

(2) The energy levels of Cu(bipy)$_3{}^{2+}$ exhibit an extraordinarily large trigonal splitting ($K = -2600$ cm^{-1}). This splitting is very likely associated with strong covalent forces, either π or σ, rather than gross distortion of the atomic framework.

(3) The anisotropy of the g tensor of Cu(bipy)$_3{}^{2+}$ observed at low temperatures is probably due to the superposition of a small rhombic component on the otherwise very strong trigonal field. However, it should be noted that the hypothesis of a strong "tetragonal" field is not absolutely invalidated by our data and a final choice between these two models will have to await further studies.

(4) Crystal intensities corrected to random orientation do not differ appreciably from those in solution for any of the tris-2,2'-bipyridine complexes thus far studied.

(5) The polarization ratios in the spectrum of Ni(bipy)$_3{}^{2+}$ are entirely different from those of other trigonal complexes (*e.g.*, oxalates, ethylenediamines) and from the theoretical ratios based on σ bonding only, indicating that the intensity probably arises in the π system.

(6) For Fe(bipy)$_3{}^{2+}$, contrary to previous reports, Dq is at least 1400 cm^{-1}, but most likely in the range 1650 to 1900 cm^{-1}.[88]

(88) Note Added in Proof.—Crosby, Perkins, and Klassen [G. A. Crosby, W. G. Perkins, and D. M. Klassen, *J. Chem. Phys.*, **43**, 1498 (1965)] have recently reported the absorption and emission spectra of Ru(bipy)$_3{}^{2+}$ in aqueous solution and in EMPA glass. In an erratum [G. A. Crosby, private communication] they have acknowledged that the band which they saw at 15,050 cm^{-1} was due to an impurity. Although we find the other relatively weak shoulder which they report at 18,550 cm^{-1} (see above), we do not agree that it is properly assigned to the $^1A_1 \rightarrow {}^1T_1$ d–d transition. The recently reported spectrum of Ru(H$_2$O)$_6{}^{2+}$ [E. E. Mercer and R. R. Buckley, *Inorg. Chem.*, **4**, 1692 (1965)] leads one to predict that the first spin-allowed band of Ru(bipy)$_3{}^{2+}$ should be much higher in energy than 18,550 cm^{-1}. Consistent with this, application of Jørgensen's empirical rule [ref 83, p 114] that Dq for a 4d^n ion is about 1.45 times Dq for a 3d^n ion to our results for Fe(bipy)$_3{}^{2+}$ gives a Dq for Ru(bipy)$_3{}^{2+}$ of *at least* 2300 cm^{-1}. This would place the $^1A_1 \rightarrow {}^3T_1$ band at 20,000 cm^{-1} and the $^1A_1 \rightarrow {}^1T_1$ band at 22,000 cm^{-1}. Considering in addition the high extinction coefficient of the 18,500 cm^{-1} band, there seems no compelling reason to assign it to a d–d transition at all.

(84) Reference 83, p 145.
(85) A. H. Ewald, R. L. Martin, I. G. Ross, and A. H. White, *Proc. Roy. Soc.* (London), **A280**, 235 (1964).
(86) C. K. Jørgensen, *Progr. Inorg. Chem.*, **4**, 92 (1962).
(87) (a) R. E. Trees, *Phys. Rev.*, **83**, 756 (1951); (b) J. S. Griffith, "The Theory of Transition Metal Ions," Cambridge University Press, 1961, p 313.